Dynamic response to electro-optical control of diamond based non-volatile photo-switch

M. Kah, N. Rouger, F. Donatini, C. Masante, F. A. Koeck, R. J. Nemanich, J. Pernot

***Abstract*— Diamond-based junction field effect transistor can be used as non-volatile photo-switches. The photo-controlled memory effect in these transistors arises from the absence of ionized nitrogen donors in the neutral region of the Ib diamond substrate gate, forming a pn junction with the p-type diamond conduction channel. In this work, we study the impact of illumination and gate designs on transistor dynamics. Electro-optical characterization, including current transients under different illumination conditions, reveal dependencies on wavelength and light power density. This study shows that optimized geometries of this device pave the way for fast switching and high-voltage applications.**

***Index Terms*— Junction field effect transistor, Diamond, Non-volatile photo switch**

I. Introduction

Non-volatile switches, and more specifically non-volatile memories, have been one of the components behind the digital revolution of recent decades. Since then, numerous technologies have been developed to improve their stability, their reliability, their robustness or their operation frequency. In parallel, new field of applications have been addressed thanks to novel materials offering specific properties. Among them, ultra wide bandgap semiconductors offer emerging opportunities due to their extremely large energy gap [1], [2], and more specifically, diamond provides outstanding properties for high power applications [3]. In this context, some of us have recently proposed a non-volatile photo-switch (NVPS) using a diamond pn junction as the gate of a diamond junction field effect transistor (JFET), with envisaged applications in the field of power electronics, quantum technologies and bio-electronics [4]. A first demonstration of the non-volatile tuning of normally on and normally off states of a deep-depletion ZrO_2/O-terminated diamond high-voltage MOSFET was recently reported [5]. The NVPS also provides complete electrical isolation of the gate when light is not supplied, thereby eliminating Miller coupling. This property is of essential importance in power electronics applications. In addition, with the growing interest in diamond-based photoconductive semiconductor switches (PCSS) thanks to sub-bandgap illumination [6], [7], diamond-based NVPSs, which are also activated by illumination rather than electrically triggered, are particularly promising in this rapidly evolving field. The integration of non-volatility in diamond devices is made possible by the generation of photo-induced carriers from deep impurities, enabling gate control. Notably, these photo-induced carriers do not contribute to p-channel conduction, a characteristic distinct from other diamond based PCSS [8] or material-based photo-switch devices such as Si [9], SiC [10], or Ga_2O_3 [11]. In this context and in order to go further, it is becoming urgent to evaluate the switching properties of these optically controlled non volatile switches to define the scope of future applications. In this study, by comparing two different diamond JFET structures, we investigate the dynamic responses of diamond-based NVPS using different excitation wavelengths and demonstrate that, thanks to optimised architectures, the achievable switching frequencies by NVPSs are consistent with high-voltage applications. To contrast with the reference diamond-based NVPS proof of concept [4], labeled as sample #1 in this work, newly proposed sample #2 undergoes optimization of the n-gate layer and gate contact to improve the dynamic performance of the NVPS under illumination.

Martin Kah and Cédric Masante are with Univ. Grenoble Alpes, CNRS, Grenoble INP, Institut Néel, 38000 Grenoble, France and LAPLACE, Université de Toulouse, CNRS, 31000 Toulouse, France

Nicolas Rouger is with LAPLACE, Université de Toulouse, CNRS, 31000 Toulouse, France

Franz A. Koeck and Robert J. Nemanich are with Arizona State University, Tempe, AZ 85281 USA. They acknowledge support by Ultra Materials for a Resilient, Smart Electricity Grid (ULTRA), an Energy Frontier Research Center (EFRC) funded by the U.S. Department of Energy, Office of Science, Basic Energy Sciences under Award # DE-SC0021230

Fabrice Donatini and Julien Pernot are with Univ. Grenoble Alpes, CNRS, Grenoble INP, Institut Néel, 38000 Grenoble, France, Corresponding authors: M.Kah (email:mryk2@cam.ac.uk) and J. Pernot (email:julien.pernot@neel.cnrs.fr). The authors are grateful to Nanofab for clean-room facilities, Juliette Letellier (Diamfab) and David Eon (Institut Néel) for fruitful discussions and French National Research Agency for funding of LSDMOSFET project: ANR-21-CE50-0036 AAPG-2021 PRCE.

II. NVPS fabrication and characteristics

Two samples were fabricated, consisting of a stack comprising an Ib HPHT substrate, (001)-oriented and 500 μm thick, provided by Sumitomo Electric, on which a boron-doped p-type epitaxial layer was deposited in the case of sample #1, and a phosphorus-doped epitaxial layer followed by a boron-doped layer in the case of sample #2 by microwave plasma assisted chemical vapor deposition. The boron doped p-type layers have been grown by Diamfab. The phosphorus doped layer has been grown at Arizona State Univ. using the process described in [12], [13]. This layer has been incorporated into the reference design to leverage the shallower phosphorus deep donor state (0.58 eV) compared to nitrogen, with the aim of increasing the generation of photo-electron in the n-type gate layer and consequently improve NVPS dynamics. The

M.Kah et al., "Dynamic response to electro-optical control of diamond based non-volatile photo-switch", IEEE Electron Device Letters, doi: 10.1109/LED.2024.3416059.
Author version - accepted manuscript https://hal.science

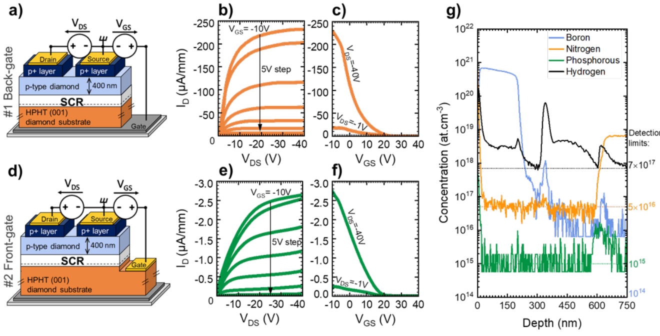

Fig. 1. a) Schematic cross section of sample $\#1$, with the gate contact fabricated on the back-side of the Ib substrate and b) sample $\#1$ output characteristic (drain current density as function of drain to source voltage for gate bias from -10 V to +20 V with 5 V steps) at room temperature and under white light illumination of 11 mW/cm^2. c) sample $\#1$ transfert characteristic (drain current density as function of gate to source voltage for drain bias of -1 V to -40 V) using same conditions as mentioned for b). d) Schematic cross section of sample $\#2$, with the gate contact fabricated on the front-side of the Ib substrate and e) sample $\#2$ output and f) transfer characteristic, using same conditions as mentioned for b). g) SIMS profile measured at the center of sample $\#2$.

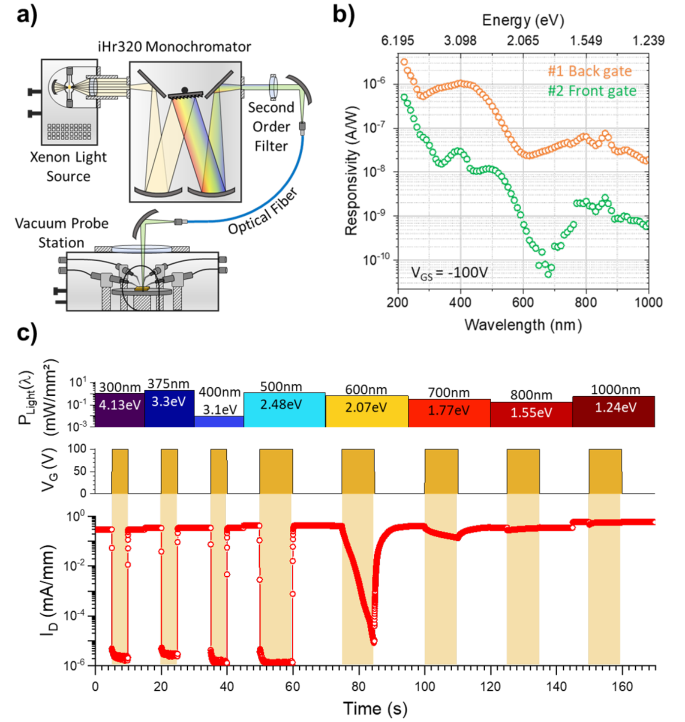

Fig. 2. a) Schematic representation of the illumination setup where poly-chromatic light is filtered in a monochromator, prior its injection inside a vacuum and temperature controlled probe station. b) Responsivity as function of the irradiation wavelength under a $V_{GS} = -100$ V. c) Sample $\#1$, drain current density at room temperature versus time under $V_{DS} = -40$ V and $V_{GS} = 0$ V (ON) or $V_{GS} = +100$ V (OFF) on the n-gate were used to effectively control the p-channel conductance under various illumination conditions.

doping level and thickness of the channel were targeted to be N$_A = 10^{17}$ cm^{-3} and 400 nm. A selectively localized heavily doped p-type diamond (10^{21} cm^{-3}) layer was deposited on the p-layer to create ohmic contacts. Then, Ti/Pt/Au (30/30/30 nm) contacts were deposited on the p+ layer. In both cases, the lightly boron-doped layer forms the channel of the JFET. The Ib HPHT substrate is the n-body of the pn back-gate junction of the JFET. In sample $\#1$, the metallic electrode of the gate contact is taken on the back side of the sample, while for sample $\#2$, on the etched front side of the sample as described in the cross sections of Fig. 1 a) and c). Quasi-static drain current versus drain source voltage measurements are reported in Fig. 1 b) and d) for different gate bias demonstrating a clear transistor control under illumination on both samples. For a drain to source length of 10 μm, the RT measured ohmic resistance are respectively 0.77 MΩ for sample $\#1$ with a gate width of 80 μm and 19 MΩ for sample $\#2$ with a gate width of 314 μm. Capacitance voltage measurements performed on a metal oxide capacitance of sample $\#1$ confirm the doping level of N$_A = 2.4 \times 10^{17}$ cm^{-3}. In case of sample $\#2$, secondary ion mass spectrometry (SIMS - Fig. 1 e)) were performed in order to determine the impurities incorporation in the epilayer during the growth process. The doping level and thickness of the boron-doped layer were below the targets, which explains the low current measured for sample $\#2$. Given a room temperature (RT) hole mobility in the p-channel of 1000 $cm^2/V.s$ relative to the doping level measured by C-V for sample $\#1$ and boron density measured by SIMS and assumed to be the doping level for sample $\#2$ [14], a three-order magnitude larger hole carrier density is evaluated for sample $\#1$ compared to sample $\#2$ at RT. In addition, the same trend was observed for the phosphorus doped layer, where the doping level and thickness were lower than targeted, making it impossible to study the effect of phosphorus.

III. Dynamic Response to Optical Excitation

Due to the large bandgap of diamond, intrinsic photo-conductivity requires photons with wavelengths below 225 nm. However, in the measurements reported in [4], given the nature of the light used, the observed photoelectric effect is attributed to extrinsic photo-conductivity, mainly related to the ionization of nitrogen donors. Extrinsic photo-conductivity produces only one type of carrier, namely electrons in the n-type substrate and holes in the p-type channel. However, the boron acceptors present in the p-channel layers are partially ionised at thermodynamic equilibrium, making the concentration of photogenerated holes negligible by comparison. To evidence the role of nitrogen in extrinsic photo-conductivity, current has been acquired as function of the photon wavelength using a dedicated setup as shown in Fig. 2 a). Cycles have been recorded separately and juxtaposed and color bars have been chosen to enlighten the higher limit of power density value for each wavelength. While illumination source is provided by a Newport 1000W, UV enhanced, Xenon Lamp, monochromatic light is obtained thanks to an Horiba iHR 320 monochromator, enabling a spectral bandwidth spanning from 200 nm (6.2 eV) to 2000 nm (0.62 eV). Light is then focused inside a probe station using off-axis parabolic mirrors and wavelength adapted optical fibers. Optical filters are used before injection to avoid second order diffraction transmission. Both samples have been maintained under vacuum, with pn

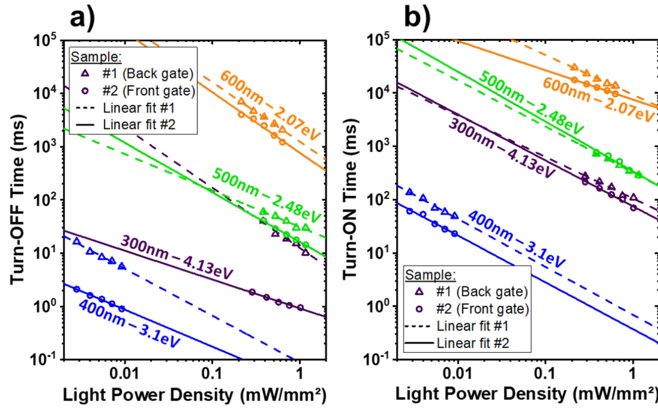

Fig. 3. a) Turn-OFF and b) Turn-ON time for both samples as function of the illumination power density for different wavelengths. Open triangles markers and open round markers stand for sample **#1** and **#2** respectively, measured data point, whereas dashed (**#1**) and solid (**#2**) lines are power law fits with an exponent ranging between 0.5 and 1.12 for each wavelength value.

junction polarized in forward (V_{GS}=-100 V) and light energy sweep is operated, starting from lowest energy toward the highest. Spectra have been acquired in separated windows and reconstructed afterward to optimize filters cascade and optical fiber transmittance range. As shown in Fig. 2 b), the pn junction responsivities, i.e. measured pn gate current density normalised by the light source power density, is not monotonous but decreases overall with the illumination wavelength. Starting around 600 nm, it aligns with the ionization energy of nitrogen donors, which is estimated to fall within the range of 1.7 eV [15] to 2.2 eV [16]. Nevertheless nitrogen optical activation is observed in both samples, and variations in photo-current is increased at higher illumination energy as supported by the increase of the optical capture cross section of substitutional nitrogen donor in respect to irradiation energy increase [16], [17].

It is particularly emphasized in Fig. 2 c) that illumination conditions have a strong impact on the JFET dynamic, i.e. turn-OFF and turn-ON durations [18]. The drain current at the turn-OFF and turn-ON times are defined as 10% and 90% of the ON-state drain current respectively. Drain current transients, in a time window triggered by the application of gate voltage bias, are recorded for various illumination conditions, such as different light power densities and energies. The turn-OFF and turn-ON time recorded for both samples are plotted in Fig. 3 as function of the light power density and for illumination wavelengths ranging from 300 nm (4.13 eV) to 600 nm (2.07 eV), to ensure the extrinsic photo-generation of free carriers in the n-type substrate. The excess photo-generated electrons are thus responsible of the turn-ON or turn-OFF time lowering, as the illumination energy rises and/or the light power density rises, an highest quantity of free electrons is generated from their fixed donor states due to the increase of the optical capture cross section [17]. Especially, according to previous work [16], the effective optical absorption cross-section of the nitrogen impurity is multiplied by 50 when the photon energy is increased from 2 eV to 4.15 eV. A linear turn-ON and -OFF time dependence is observed versus the light power density for each wavelength. An equivalent resistor-capacitor (RC) circuit with a typical time constant τ [19] is proposed to model the gate transient:

$$\tau = \frac{t_n}{e\mu_n(n_0 + \Delta n_{ph})} \times \frac{\epsilon_{Diam}\epsilon_0}{W_{SCR}} \quad (1)$$

where t_n is the thickness of the n-type layer, e, the elementary charge, μ_n the electron mobility in Ib diamond substrate assumed to fall around 70 $cm^2/V.s$ for a donor concentration $N_D \approx 10^{19}$ cm^{-3} [20], n_0 the free electron density at equilibrium, Δn_{ph} the photo-generated electrons ionized by illumination, $\epsilon_{Diam}\epsilon_0$ the diamond permittivity, and W_{SCR} the space charge region (SCR) width. The first term of the right part of the equation corresponds to the resistance by unit of area of the $n-$type substrate R_{SUB} and second term to the SCR capacitance by unit of area C_{SCR}. From R_{SUB} extracted from the serial resistance of the pn junction of the gate measured under illumination (see for example sample #1 in ref [4]) and assuming μ_n value given above, Δn_{ph} is estimated to be in the range and not lower than 10^{11} cm^{-3}. Since $n_0 \approx 10^2$ cm^{-3} can be evaluated at RT from the charge neutrality equation, one can assume $(n_0 + \Delta n_{ph}) \approx \Delta n_{ph}$. The sample with the gate contacts, positioned on the front-side of the Ib substrate serving as the JFET gate, exhibit a turn-OFF time faster than its counterpart on the back-side of the Ib substrate under constant monochromatic illumination, for example 5 times faster at 400 nm and 0.01 mW/mm^2 (τ = 880 μs and τ = 5.6 ms respectively). Considering the equivalence of the substrate resistivity under illumination for the two samples, despite differences in geometric aspect ratios; whereas sample #1 requires the entire thickness of the substrate to be considered, the lateral distance to be taken into account for sample #2 requires a more complex calculation, finally revealing a significant drop in the R_{SUB} on sample #2 compared with sample #1. The shorter commutation time due to the lower R_{SUB} on sample #2 is also observed to a lesser extent for the turn-ON time of the transistor. It is noteworthy that the observed time constants in the analysis fall short of the stringent specifications set by the power electronics application. Nevertheless, emphasis must be placed on the fact that the analysis presented in this study provides a foundational framework for future optimization, thus holding the promise of yielding devices capable of meeting and competing within the standards of the targeted market, with added value like galvanic insulation of the non-illuminated gate.

IV. Conclusion

This study presents an analysis and modelling of the dynamic switching properties of non-volatile photo-switches based on a diamond JFET. The gate contacts, positioned on the front surface of the Ib substrate acting as a JFET gate, enabled the turn-off and turn-on times to be reduced under constant illumination. Wavelength and optical excitation power density are proving to be key points for future devices with optimised architectures capable of operating at high frequency and high voltage.

M.Kah et al., "Dynamic response to electro-optical control of diamond based non-volatile photo-switch", IEEE Electron Device Letters, doi: 10.1109/LED.2024.3416059.
Author version - accepted manuscript https://hal.science

References

[1] J. Y. Tsao, S. Chowdhury, M. A. Hollis, D. Jena, N. M. Johnson, K. A. Jones, R. J. Kaplar, S. Rajan, C. G. Van de Walle, E. Bellotti, C. L. Chua, R. Collazo, M. E. Coltrin, J. A. Cooper, K. R. Evans, S. Graham, T. A. Grotjohn, E. R. Heller, M. Higashiwaki, M. S. Islam, P. W. Juodawlkis, M. A. Khan, A. D. Koehler, J. H. Leach, U. K. Mishra, R. J. Nemanich, R. C. N. Pilawa-Podgurski, J. B. Shealy, Z. Sitar, M. J. Tadjer, A. F. Witulski, M. Wraback, and J. A. Simmons, "Ultrawide-bandgap semiconductors: Research opportunities and challenges," *Advanced Electronic Materials*, vol. 4, no. 1, p. 1 600 501, 2018. DOI: 10.1002/aelm.201600501.

[2] M. Higashiwaki, R. Kaplar, J. Pernot, and H. Zhao, "Ultrawide bandgap semiconductors," *Applied Physics Letters*, vol. 118, no. 20, 2021. DOI: 10.1063/5.0055292.

[3] N. Donato, N. Rouger, J. Pernot, G. Longobardi, and F. Udrea, "Diamond power devices: State of the art, modelling, figures of merit and future perspective," *Journal of Physics D: Applied Physics*, vol. 53, no. 9, p. 093 001, 2019. DOI: 10.1088/1361-6463/ab4eab.

[4] C. Masante, M. Kah, C. Hébert, N. Rouger, and J. Pernot, "Non-Volatile Photo-Switch Using a Diamond pn Junction," en, *Advanced Electronic Materials*, vol. 8, no. 1, p. 2 100 542, Jan. 2022, ISSN: 2199-160X, 2199-160X. DOI: 10.1002/aelm.202100542.

[5] B. Soto, M. Couret, J. Cañas, A. Castelan, N. Rouger, D. Araujo, M. P. Villar, and J. Pernot, "Non-volatile tuning of normally-on and off states of deep depletion ZrO2/O-terminated high voltage diamond MOSFET," *Diamond and Related Materials*, vol. 134, p. 109 802, 2023. DOI: 10.1016/j.diamond.2023.109802.

[6] D. L. Hall, L. F. Voss, P. Grivickas, M. Bora, A. M. Conway, P. Ščajev, and V. Grivickas, "Photoconductive switch with high sub-bandgap responsivity in nitrogen-doped diamond," *IEEE Electron Device Letters*, vol. 41, no. 7, pp. 1070–1073, 2020. DOI: 10.1109/LED.2020.2999821.

[7] K. Woo, M. Malakoutian, B. A. Reeves, and S. Chowdhury, "A study on sub-bandgap photoexcitation in nitrogen-and boron-doped diamond with interdigitated device structure," *Applied Physics Letters*, vol. 120, no. 11, 2022. DOI: 10.1063/5.0083710.

[8] Z. Han, J. Lee, S. Messing, T. Reboli, A. Mironov, and C. Bayram, "High current density diamond photoconductive semiconductor switches with a buried, metallic conductive channel," *IEEE Electron Device Letters*, pp. 1–1, 2024. DOI: 10.1109/LED.2024.3387325.

[9] J. C. Koo, G. M. McWright, M. D. Pocha, and R. B. Wilcox, "Low leakage 10,000-v silicon photoconductive switch," *Appl. Phys. Lett.; (United States)*, vol. 45:10, Nov. 1984. DOI: 10.1063/1.95043.

[10] Z. Feng, C. Luan, L. Xiao, Y. Li, H. Sha, X. Sun, X. Chen, X. Xu, and H. Li, "Performance of a novel rear-triggered 4h-sic photoconductive semiconductor switch," *IEEE Transactions on Electron Devices*, vol. 70, no. 2, pp. 627–632, 2023. DOI: 10.1109/TED.2022.3227889.

[11] K. M. Dowling, B. Chatterjee, S. Ghandiparsi, Q. Shao, J. Varley, J. D. Schneider, C. Chapin, M. S. Gottlieb, L. Leos, M. Sword, S. Harrison, and L. Voss, "Evaluation of fe-ga2o3 for photoconductive semiconductor switching," *IEEE Transactions on Electron Devices*, vol. 71, no. 3, pp. 1535–1540, 2024. DOI: 10.1109/TED.2024.3352528.

[12] M. Dutta, F. A. Koeck, W. Li, R. J. Nemanich, and S. Chowdhury, "High voltage diodes in diamond using (100)-and (111)-substrates," *IEEE Electron Device Letters*, vol. 38, no. 5, pp. 600–603, 2017. DOI: 10.1109/LED.2017.2681058.

[13] F. A. Koeck, M. Benipal, and R. J. Nemanich, "Electrical contact considerations for diamond electron emission diodes," *Diamond and Related Materials*, vol. 101, p. 107 607, 2020. DOI: 10.1016/j.diamond.2019.107607.

[14] P.-N. Volpe, J. Pernot, P. Muret, and F. Omnès, "High hole mobility in boron doped diamond for power device applications," *Applied Physics Letters*, vol. 94, no. 9, p. 092 102, Mar. 2009, ISSN: 0003-6951. DOI: 10.1063/1.3086397.

[15] B. B. Li, M. C. Tosin, A. C. Peterlevitz, and V. Baranauskas, "Measurement of the substitutional nitrogen activation energy in diamond films," en, *Applied Physics Letters*, vol. 73, no. 6, pp. 812–814, Aug. 1998. DOI: 10.1063/1.122010.

[16] W. J. P. V. Enckevort and E. H. Versteegen, "Temperature dependence of optical absorption by the single-substitutional nitrogen donor in diamond," en, *Journal of Physics: Condensed Matter*, vol. 4, no. 9, pp. 2361–2373, Mar. 1992. DOI: 10.1088/0953-8984/4/9/028.

[17] M. Nesládek, K. Meykens, K. Haenen, L. Stals, T. Teraji, and S. Koizumi, "Low-temperature spectroscopic study of n-type diamond," *Physical Review B*, vol. 59, no. 23, p. 14 852, 1999. DOI: 10.1103/PhysRevB.59.14852.

[18] J. L. Moll, "Large-signal transient response of junction transistors," *Proceedings of the IRE*, vol. 42, no. 12, pp. 1773–1784, 1954. DOI: 10.1109/JRPROC.1954.274798.

[19] J. Moll, S. Krakauer, and R. Shen, "PN junction charge-storage diodes," *Proceedings of the IRE*, vol. 50, no. 1, pp. 43–53, 1962. DOI: 10.1109/JRPROC.1962.288273.

[20] J. Pernot and S. Koizumi, "Electron mobility in phosphorous doped {111} homoepitaxial diamond," *Applied Physics Letters*, vol. 93, no. 5, 2008. DOI: 10.1063/1.2969066.

M.Kah et al., "Dynamic response to electro-optical control of diamond based non-volatile photo-switch", IEEE Electron Device Letters, doi: 10.1109/LED.2024.3416059.
Author version - accepted manuscript https://hal.science